NASA TN D-175

TECHNICAL NOTE
D-175

DYNAMIC-MODEL INVESTIGATION OF THE DAMPING OF FLAPWISE BENDING MODES OF TWO-BLADE ROTORS IN HOVERING AND A COMPARISON WITH QUASI-STATIC AND UNSTEADY AERODYNAMIC THEORIES

By Milton A. Silveira and George W. Brooks

Langley Research Center
Langley Field, Va.

NATIONAL AERONAUTICS AND SPACE ADMINISTRATION
WASHINGTON
December 1959

NATIONAL AERONAUTICS AND SPACE ADMINISTRATION

TECHNICAL NOTE D-175

DYNAMIC-MODEL INVESTIGATION OF THE DAMPING OF FLAPWISE BENDING MODES OF TWO-BLADE ROTORS IN HOVERING AND A COMPARISON WITH QUASI-STATIC AND UNSTEADY AERODYNAMIC THEORIES*

By Milton A. Silveira and George W. Brooks

SUMMARY

The objective of this report is to present the findings of a systematic investigation of the deficiency in damping of rotor blades operating at low, rotor inflow velocities. The results of a dynamic-model study of the damping of symmetric flapwise bending modes of a two-blade teetering and flapping rotor are presented and compared with damping values calculated from both quasi-static and unsteady aerodynamic theories. Structural and aerodynamic damping values are given for the second and third modes for each of two collective pitch angles for hovering at low rotor inflow velocities.

The results show that, under conditions of negligible inflow, the total damping, when plotted as a function of the ratio of blade bending frequency to rotor speed, fluctuates, in general, between upper and lower bounds given by combined quasi-static aerodynamic and structural damping and by structural damping, respectively. The lower values of total damping occur at frequency ratios just below even integral values and indicate that, under conditions of low rotor inflow, the contributions of aerodynamic damping in these cases are negligible.

The comparison of the experimental results with those of existing two-dimensional idealized theory shows that the trends predicted by the theory are essentially realized; but some variations exist which are probably due to the effects of slipstream contraction, rotation, and possibly other factors which include the three-dimensional aspects of the flow.

---

*Part of the information presented herein was offered by Milton A. Silveira as a thesis entitled "The Damping of Flapwise Bending Modes of Two-Blade Rotors in Hovering" in partial fulfillment of the requirements for the degree of Master of Science in Aeronautical Engineering, University of Virginia, Charlottesville, Virginia, June 1959.

INTRODUCTION

During the operation of various types of rotors under conditions of hovering and forward flight, the rotors are subjected to periodic aerodynamic and dynamic loads. These applied loads may be resolved by the methods of Fourier series into various harmonic components which have frequencies equal to the integral multiples of the rotor speed. The natural frequencies of the blades themselves are also dependent on the rotor speed because of the centrifugal stiffening effects. The results of these combined effects are such that as the rotor speed is varied, the frequencies of the harmonic components of the aerodynamic loading may become resonant or near resonant with one or more of the natural frequencies of the blades. Under such conditions, the aerodynamic and structural damping of the blades is of fundamental importance in maintaining acceptable levels of blade deflections and associated blade stresses.

The results of the idealized two-dimensional theories of references 1 and 2 show that the aerodynamic damping of both blade bending and torsion deformations are modified appreciably from the values predicted by quasi-static considerations if the wake effects are included. It is shown, under conditions involving low rotor inflow velocities, that the effective aerodynamic damping may be substantially reduced when the frequencies of the blade vibrations are integral multiples of the rotor speed.

The earliest experimental recognition of the phenomenon predicted by the aforementioned theories was encountered in the so-called "wake" flutter of propeller and rotor blades (see refs. 3 and 4) wherein the blade deformations are principally torsional. More recently experimental agreement with the predicted trends of a deficiency in damping of blade flapwise bending deformations has also been found for a rotor having a single flapping blade (ref. 5).

The present report presents the results of a systematic experimental study of the damping of blade flapwise bending deformations for both the teetering and flapping rotor configurations with blades dynamically scaled to be structurally representative of current designs. Experimental values for both aerodynamic and structural damping are presented and compared with the results obtained from both quasi-static and unsteady aerodynamic theories.

SYMBOLS

b	blade half-chord
F'	real part of the modified lift-deficiency function for rotors (ref. 1)
h	vertical distance between successive rows of vorticity
m	mass of blade per unit length
n	number of cycles
R	rotor radius
r	radial position of arbitrary blade element
U	mean induced velocity through the rotor
x_n	amplitude of nth oscillation of decay
x_o	amplitude of initial oscillation of decay
γ	line strength of continuously distributed vorticity
δ	damping factor, $\frac{1}{n} \log_e \frac{x_o}{x_n}$
δ_o	damping factor, nonrotating value
θ	collective pitch angle of rotor blades
ρ	air density
ϕ	bending mode shape
Ω	rotational frequency of rotor
ω	rotor-blade flapwise bending natural frequency
ω_o	rotor-blade flapwise bending natural frequency, nonrotating value

APPARATUS AND TESTS

Description of Apparatus

Sketches of the apparatus used for the teetering and flapping rotors are shown in figures 1 and 2, respectively. For the teetering rotor, the rotor was mounted at the free end of a cantilever beam which was excited by an electronic shaker as shown in figure 1. For the flapping rotor, the free end of the beam was fixed and the shaker was mounted above the rotor to shake the blades directly as shown in figure 2. When the beam was mounted as a cantilever, small viscous dampers were attached to the beam to obtain near-critical damping of the beam vibrations upon removal of the exciting force. The length of the cantilever beam was also varied during particular phases of the test to eliminate large beam deflections and severe coupling of its natural frequencies with those of the blades.

It was concluded, after several tries, that the pin-end bending modes for the flapping rotor could not be excited with sufficient clarity by shaking the support beam to permit an accurate evaluation of the damping. Consequently, a very lightweight shaker was mounted above the rotor in order to excite the blades directly as shown in figure 2. The blades were excited through two flexible wires attached to the shaker by means of a small bar which was free to rotate about the shaker driving shaft.

The rotor was driven by a small commercial air motor mounted below the beam and connected to the rotor shaft through a right-angle gear box. A complete description of the pylon assembly is given in reference 6.

The hubs for the two configurations are shown in figures 3 and 4. Both rotors employed the same blades which are described in detail in reference 6 and are shown in figure 5. A rotor diameter of 66 inches and a solidity of 0.04 were maintained with each configuration. The rotor blades had an NACA 0015 airfoil section, a uniform 2.062-inch chord, and were constructed of solid balsa glued to an inlaid solid-aluminum spar. They were dynamically scaled to possess the flapwise bending properties (mass and stiffness) representative of current helicopter-rotor blade designs.

The teetering-rotor hub, shown in figure 3, was of a conventional configuration and consisted of a rigid unit free to pivot about a horizontal pin at the top of the rotor shaft.

The flapping-rotor hub, shown in figure 4, utilized short lengths of 1/16-inch-diameter aircraft cable to act as flapping hinges and retention straps. The blade-retention blocks are clamped to the two lengths

of aircraft cable. An arm extends below the blade-root fitting to act as the blade-droop stop.

Instrumentation

The instrumentation of the model consisted of electrical resistance-wire strain gages mounted on the blades and near the root of the cantilever beam. An instantaneous indication of rotor speed was obtained by means of a tachometer generator and Stroboconn, and a 1-per-revolution signal was used for recording purposes. All signals were recorded by an oscillograph, a sample record of which is shown in figure 6.

Test Procedure

The collective pitch angle of the blades was set and locked before each test. Prior to obtaining any values of the blade damping, the thrust of the rotor throughout the range of operating speeds was measured by means of the calibrated beam bending gage.

The blade-damping data presented were obtained by setting the rotor speed at the value desired and by varying the frequency of the exciting force applied by the shaker to secure a maximum deflection of the blades in the prescribed mode (resonance). This procedure was used to maximize blade response and to minimize any transient state between the frequency of the forced and free vibration of the blade. When the aforementioned conditions of resonance were obtained, logarithmic decrements were recorded of the decaying oscillation of the free vibrations of the blade by suddenly removing the exciting force. For each value of the frequency ratio (ratio of blade natural frequency to rotor speed), at least four decrements were obtained and, consequently, four values of the damping factor were derived.

The use of the logarithmic-decrement method, in contrast with the forced-response method, in obtaining damping introduces a transient factor. In the logarithmic-decrement method, the strength of the vorticity which is continuously shed by a blade element and lies in the near wake is dependent on the amplitude of the blade oscillation and, therefore, diminishes as the amplitude diminishes. In the forced-response method, the amplitude of the oscillation is steady and the strength of the shed vorticity in the near wake is uniform. The data presented in reference 5 were obtained by both methods and show that the results obtained by the two methods are essentially the same. It is concluded, therefore, that the effect of the decay in the vortex strength immediately behind the blade due to the logarithmic decay of the blade oscillations does not have a substantial effect on the overall aerodynamic damping of the blade.

The structural damping of the blades was also measured by the logarithmic-decrement method. In order to obtain the damping at zero rotor speeds, the blades were supported at the node points of the respective modes by soft rubber bands.

The effect of rotor speed on the structural damping of the teetering rotor is treated analytically in a subsequent section entitled "Analysis and Presentation of Data." However, because of the nature of the flapping hinge, it was felt that an experimental investigation of the variation of structural damping with rotor speed was necessary. This effect was measured by mounting a rotor in a vacuum chamber (with use of the same flapping hinges and blade attachments but different blades) and by measuring the damping by the logarithmic-decrement method throughout the rotor speed range.

Range of Tests

Damping values were obtained for the second and third elastic bending modes for the teetering and flapping configurations over a range of rotor speeds bounded at the lower end by droop-stop banding and at the upper end by the design value of centrifugal forces. The test ranges of rotor speed are given in figures 7 and 8. These figures also show the values of the ratio of the blade natural frequency to rotational frequency obtained for the respective modes within the test range of rotor speed. A small change in rotor speed at the lower rotor speeds results in a large change in the value of the frequency ratio ω/Ω; whereas at high rotor speeds, a large change in rotor speed is required to obtain a small change in the value of the frequency ratio. Tests for the first modes were not included in this investigation because the range of possible rotor speeds did not include a sufficient range of the frequency ratio to be of interest.

During the investigation, data were obtained for nominal collective pitch-angle settings of 0° and 3°. From these nominal settings, it was necessary to vary the pitch angle of one blade slightly to obtain good blade tracking. Because of these adjustments and the inaccuracies of precisely defining the collective pitch angles of small blades, it was decided that a measure of the rotor thrust would provide a more realistic evaluation of actual rotor operating conditions, especially with regard to the conditions of rotor inflow. Consequently, prior to obtaining the damping data, the thrust was measured as a function of rotor speed for each of the two nominal values of collective pitch angle, and the results are presented in figures 9 and 10. These figures show that the blade angle of attack is reduced somewhat as the rotor speed is increased. This effect is more pronounced in figure 10 where the thrust is given for the flapping blade. In either case, the lower value for the collective pitch angle was selected so as to yield negligible thrust near the

maximum rotor speed. The nominal pitch angles are then used to identify the respective data presented in figures 11 to 15.

ANALYSIS AND PRESENTATION OF DATA

General Discussion

The analysis and presentation of the results of this investigation are described in some detail in the sections which follow. Both measured and calculated damping factors are presented and compared. The results are presented in figures 11 to 15. The coverage and order of presentation consist of measured and calculated values of the structural damping, the summation of the structural damping and the calculated quasi-static aerodynamic damping (wake effects ignored), the summation of the structural damping and the calculated unsteady aerodynamic damping (wake below and immediately behind the blade considered), and the summation of the structural damping and calculated unsteady aerodynamic damping (wake below the rotor ignored, wake immediately behind the blade considered).

Measured Values of Blade Total Damping

The measured damping factors presented were derived from the following relation:

$$\delta = \frac{1}{n} \log_e \frac{x_o}{x_n}$$

The amplitude x_o may be taken for any cycle after the shaker force is terminated and the blade motion assumes a damped-free vibration. The amplitude x_n is then the amplitude of the nth cycle after that taken as x_o.

A typical plot of the data, as read from the records, is presented in figure 11. Because of the transmission of the data through sliprings and other factors, some scatter of the data was experienced; but, by deriving several damping factors for each test point and by using numerous test points, the general trends of the damping factors were well defined. In general, the amount of scatter was less for the third modes than for the second modes and was less for the teetering rotor than for the flapping rotor.

After the data were plotted, curves were faired through the data points as shown in figure 11, and these curves are presented in figures 12

and 13 for the teetering rotor and in figures 14 and 15 for the flapping rotor.

Structural Damping

In order to obtain a ready comparison of the experimental damping factors measured during this investigation with those predicted by theory, it was necessary to establish the value of the structural damping for each configuration and condition tested since the structural damping is added to the calculated aerodynamic damping in each case. The structural damping at zero rotor speed was readily measured as previously described in the section entitled "Test Procedure"; however, the variation of structural damping with rotor speed posed some difficulties.

In the consideration of the blade as a generalized mass-spring-damper system, the structural damping force is given as the product of the structural damping coefficient and the generalized spring constant. If the usual assumption is made that the structural damping force is dependent only on the properties of the structure and the mode of deformation, then the effective structural-damping coefficient decreases as the rotor speed increases because of the increase in the generalized spring constant. The effective structural-damping coefficient is then given by

$$\delta = \delta_0\left(\frac{\omega_0}{\omega}\right)^2$$

where δ_0 and ω_0 are the appropriate values for the given mode at $\Omega = 0$. This assumption appears to be appropriate for the teetering rotor since the blade-root fittings and hub constitute a continuous structure, and it was used to derive the structural-damping curves and the structural-damping component of the quasi-static and unsteady aerodynamic curves of figures 12 and 13. Test results for the flapping bodies showed that for some conditions, if the $\delta = \delta_0\left(\frac{\omega_0}{\omega}\right)^2$ relationship was applied, the total damping appeared to be less than the calculated structural damping. Consequently, separate tests were made on a similar flapping rotor in a near vacuum to determine the variation of structural damping with rotor speed, and the results were used to obtain the curves for structural damping presented in figures 14 and 15. These values were also used as the structural damping components in the determination of the quasi-static and unsteady-aerodynamic-damping curves for the flapping rotor.

The variation of structural damping with amplitude of the blade vibrations was investigated to determine the extent of the variation. It was found that, within the range of amplitudes used in exciting the blades, the variation of structural damping with amplitude was insignificant and, therefore, no attempt was made to retain a constant initial amplitude of the blade response.

The results obtained from several tests of a conventional, fully articulated, flapping rotor showed that the friction of the flapping hinge (a brass pin and steel bushing) increased substantially with rotor speed. In fact, at the higher rotor speeds this friction was such that it masked out the deficiency in aerodynamic damping associated with the wake, and at all rotor speeds the friction was unknown and could not be readily determined. It was because of the excessive friction in this rotor that the flapping rotor with flexible straps was designed and tested. Only a limited amount of data was taken for the fully articulated rotor, and becase of the uncertainties of the results, these data are not presented.

With regard to the friction of the fully articulated hinged rotor, some further remarks seem pertinent. Experience with dynamic models suggests that the relative magnitude of friction forces generally increases as the size of the model is reduced. This is brought about by a combination of factors which include poor lubrication, lower bearing efficiencies, and the necessity for change in bearing types. As a result of these factors, it is likely that a full-scale helicopter rotor would experience lower relative friction forces than a smaller model; but even so, it is also likely that the structural damping of the vibration modes of blades having flapping hinges to transmit centrifugal forces is higher than that for a teetering rotor.

Quasi-Static Damping

The aerodynamic components of the quasi-static damping values presented in figures 12 to 15 were calculated by employing the generalized mass-spring-damper concept (ref. 5) wherein each mode of the blade is treated as an equivalent one-degree-of-freedom system. In this system, since the blades are of uniform rectangular plan form, the damping factor is given by

$$\delta_s = \frac{\pi}{\frac{\omega_s}{\Omega} m} \rho c l_\alpha b \frac{\int_0^R \phi_s^2 r \, dr}{\int_0^R \phi_s^2 \, dr}$$

where the subscript s denotes the mode, shape of which is denoted by ϕ. The value of the slope of the lift curve c_{l_α} is assumed to be uniform and equal to 5.7 per radian.

In order to determine the curves presented in figures 12 to 15, the values of the aerodynamic components thus determined are added to the appropriate values of structural damping.

Unsteady Damping

In addition to the experimental, structural, and quasi-static damping curves, the damping factors which include the wake effects were also calculated and are presented in figures 12 to 15. These calculations are based on the results of reference 1 and consist of modifying the aerodynamic components of the quasi-static damping by a factor F' which is a function of the inflow velocity through the rotor, the frequency ratio ω/Ω, and the reduced frequency $b\omega/r\Omega$. With reference to any one of figures 12 to 15 there is a unique rotor speed Ω corresponding to each value of ω/Ω. Then, from the appropriate figure, 8 or 9, the appropriate value of rotor thrust is obtained. By using this value of thrust and assuming that the inflow velocity through the rotor is uniform, the inflow velocity is determined. The reduced frequency is then calculated for a representative blade station ($r = 0.75R$), and the value of F' is calculated from reference 1. The curves presented in figures 12 to 15 are then obtained by multiplying the appropriate value of the aerodynamic component of the quasi-static damping by F' and adding the corresponding value of structural damping. It may be noted that in reference 1 the theoretical slope of the lift curve is given as $2\pi F'$; whereas in the present report the effective slope is taken as $5.7F'$. The latter value is believed to be more appropriate for helicopter blades.

The oscillations in the unsteady-damping curves may be briefly explained by reference to the aerodynamic model shown in figure 16. In this model, certain idealizations of the flow problem are made in order to make the problem mathematically tractable. These are pointed out in the remarks which follow and should be kept in mind in the discussion.

First, a section of a blade which lies between two concentric cylinders is considered, and it is assumed that the factors which influence the aerodynamics of the section have sufficiently small spanwise variations that the flow problem is two dimensional. Secondly, although in the actual case the blade element is moving along a curved path, in the theoretical model it is assumed that the effect of this curvature is small and the curved path is replaced by a straight line. A third idealization is employed wherein the induced velocity of the wake is assumed to be sufficiently small that the wake shed from the blades lies

in planes which are parallel to each other and normal to the rotor axis; or, in other words, the helix angle of the wake is neglected. A fourth idealization is the assumption that only that portion of the wake which lies within a small azimuth angle on either side of the blade element is effective in determining the aerodynamics of the blade. This assumption permits the limits of the integrals for the wake elements below the rotor to be considered infinite.

The fluctuations in the strength of the line vorticity which lies in the wake below the rotor plane are dependent on the number of blades, the value of ω/Ω, and whether the blade vibrations are symmetrical or antisymmetrical. The vertical distance between the rows of vorticity h (shown in fig. 16 as a dimensionless quantity) is dependent on the inflow velocity, the number of blades, and the rotor speed. The figure presented corresponds to the condition of the tests (two-blade rotor with symmetrical oscillations) and depicts conditions wherein ω/Ω is either an even integral or an odd integral. When ω/Ω is an even integral, all rows of vorticity are of the same phase and reinforce each other to produce an induced-velocity field in the plane of the rotor in phase with the blade motions. Thus, the velocity of the blade relative to the surrounding air is reduced and the effective damping of the blade oscillations is diminished. On the other hand, when ω/Ω is an odd integral, the tendency of the rows of vorticity in the wake is to cancel each other, and the damping is expected to approach the quasi-static value.

As the vertical distance between successive rows of vorticity becomes very large, only the vorticity immediately behind the rotor is significant. This situation, which corresponds to the curves in figures 12 to 15 labeled $h = \infty$, is equivalent to that of an oscillating wing as treated by the classical unsteady aerodynamic theories such as that presented in reference 7.

DISCUSSION OF RESULTS

The experimental curves for both rotor configurations and pitch angles presented in figures 12 to 15 exhibit a substantial reduction in the damping factor at frequency ratios usually somewhat below the even integral values. In general, the curves for quasi-static damping and structural damping essentially form the upper and lower bounds to the experimental curves for conditions of negligible inflow.

A comparison of the experimental damping curves with those derived on the basis of the unsteady aerodynamic theory of reference 1 shows that the trends predicted by the theory, even though it is highly idealized, are substantiated by the experimental results, and in most cases,

the agreement between numerical values is good. The troughs in the curves occur somewhat below the even-integral frequency ratio predicted by the theory. The troughs for the higher pitch angles occur nearer to the even-integral frequency ratios than those for the nominal blade-pitch-angle settings of 0°. The occurrence of the troughs before the integral values is probably due to rotation of the slipstream, a factor not treated in the development of the theory of reference 1. The general shapes of the troughs for the experimental damping factors are rounded in contrast with the sharp cusplike troughs sometimes predicted by the theory. This may be due to three-dimensional effects resulting from the differences in the inflow angles and the ratio $b\omega/r\Omega$ over the blade span.

The amplitudes of the oscillations of the experimental damping factors decreased as the frequency ratio increased (lower rotor speed). This is consistent with theory in that the quasi-static damping approaches the structural damping at low rotational frequencies.

The experimental data indicate that the amplitude of oscillation of the damping factor for the blade pitch angles of $\theta = 0^\circ$ is greater than that for $\theta = 3^\circ$. This trend is also in agreement with the general trend predicted by the theory: that a reduction in inflow (thrust) is accompanied by a reduction in damping at the troughs and by an increase in damping at the peaks. A fact of particular interest in regard to this trend, and which is generally true for all cases except for the second mode for the teetering rotor, is that the oscillation of the damping factor as the effective pitch angle is increased seems to converge to some value considerably below the quasi-static value. This value would correspond to a large pitch angle where the shed vortex was infinitely far below the rotor ($h = \infty$). This trend is also consistent with the theory of reference 1, which, in this case, reduces to the results of the classical theory for the aerodynamic forces on oscillating wings (ref. 7).

The results of the experimental investigation reported herein clearly show that substantial reductions in the effective aerodynamic damping occur when the rotor is operating under conditions of low inflow and occur particularly at rotor speeds where the bending frequencies of the blades are slightly below some integral multiples of the rotor speed (the important integral multiples being dependent on the number of blades, etc., as previously pointed out). The results further show that the trends coincide in principle with those of the theory, but they seem to be modified by the existence of the effects of slipstream rotation and three-dimensional variations in the flow about the blade over the length of the span.

SUMMARY OF RESULTS

An investigation of the damping of the flapwise symmetrical elastic bending modes of a dynamically scaled two-blade teetering rotor and a two-blade flapping rotor during conditions of low inflow in hovering has been conducted, and the results may be summarized as follows:

1. A comparison of the results with existing theory indicates that the trends predicted by the theory, even though it is highly idealized, are essentially realized; but, some differences exist which are probably associated with the rotation of the slipstream and three-dimensional-flow conditions not treated in the development of the theory.

2. A substantial fluctuation of the aerodynamic damping of the blade motions associated with flapwise elastic bending occurs as the ratio of blade oscillatory frequency to rotational frequency ω/Ω is varied, and the value of the damping factors oscillate essentially between the structural and quasi-static values.

3. The minimum values of the damping factor for the two-blade rotors, bending in symmetrical modes, occur just prior to the even integral values of ω/Ω.

4. The results show that as the rotor inflow velocity is increased the fluctutation in damping decreases. In the limit, as the inflow becomes sufficiently large, the vorticity below the rotor is swept away and only the wake immediately behind the blade has a significant effect on the blade damping. In this case, the damping converges to a value which is below the quasi-static value as predicted by the existing two-dimensional unsteady aerodynamic theory, which, in this case, reduces to the classical theory for aerodynamic forces on an oscillating wing.

Langley Research Center,
National Aeronautics and Space Administration,
Langley Field, Va., August 31, 1959.

REFERENCES

1. Loewy, Robert G.: A Two-Dimensional Approximation to the Unsteady Aerodynamics of Rotary Wings. Jour. Aero. Sci., vol. 24, no. 2, Feb. 1957, pp. 81-92, 144.

2. Timman R., and Van de Vooren, A. I.: Flutter of a Helicopter Rotor Rotating in Its Own Wake. Jour. Aero. Sci., vol. 24, no. 9, Sept. 1957, pp. 694-702.

3. Theodorsen, Theodore, and Regier, Arthur A.: Effect of the Lift Coefficient on Propeller Flutter. NACA WR L-161, 1945. (Formerly NACA ACR L5F30.)

4. Brooks, George W., and Baker, John E.: An Experimental Investigation of the Effect of Various Parameters Including Tip Mach Number on the Flutter of Some Model Helicopter Rotor Blades. NACA TN 4005, 1958. (Supersedes NACA RM L53D24.)

5. Daughaday, Hamilton, DuWaldt, Frank, and Gates, Charles: Investigation of Helicopter Blade Flutter and Load Amplification Problems. Jour. Am. Helicopter Soc., vol. 2, no. 3, July 1957, pp. 27-45.

6. Silveira, Milton A., and Brooks, George W.: Analytical and Experimental Determination of the Coupled Natural Frequencies and Mode Shapes of a Dynamic Model of a Single-Rotor Helicopter. NASA MEMO 11-5-58L, 1958.

7. Theodorsen, Theodore: General Theory of Aerodynamic Instability and the Mechanism of Flutter. NACA Rep. 496, 1935.

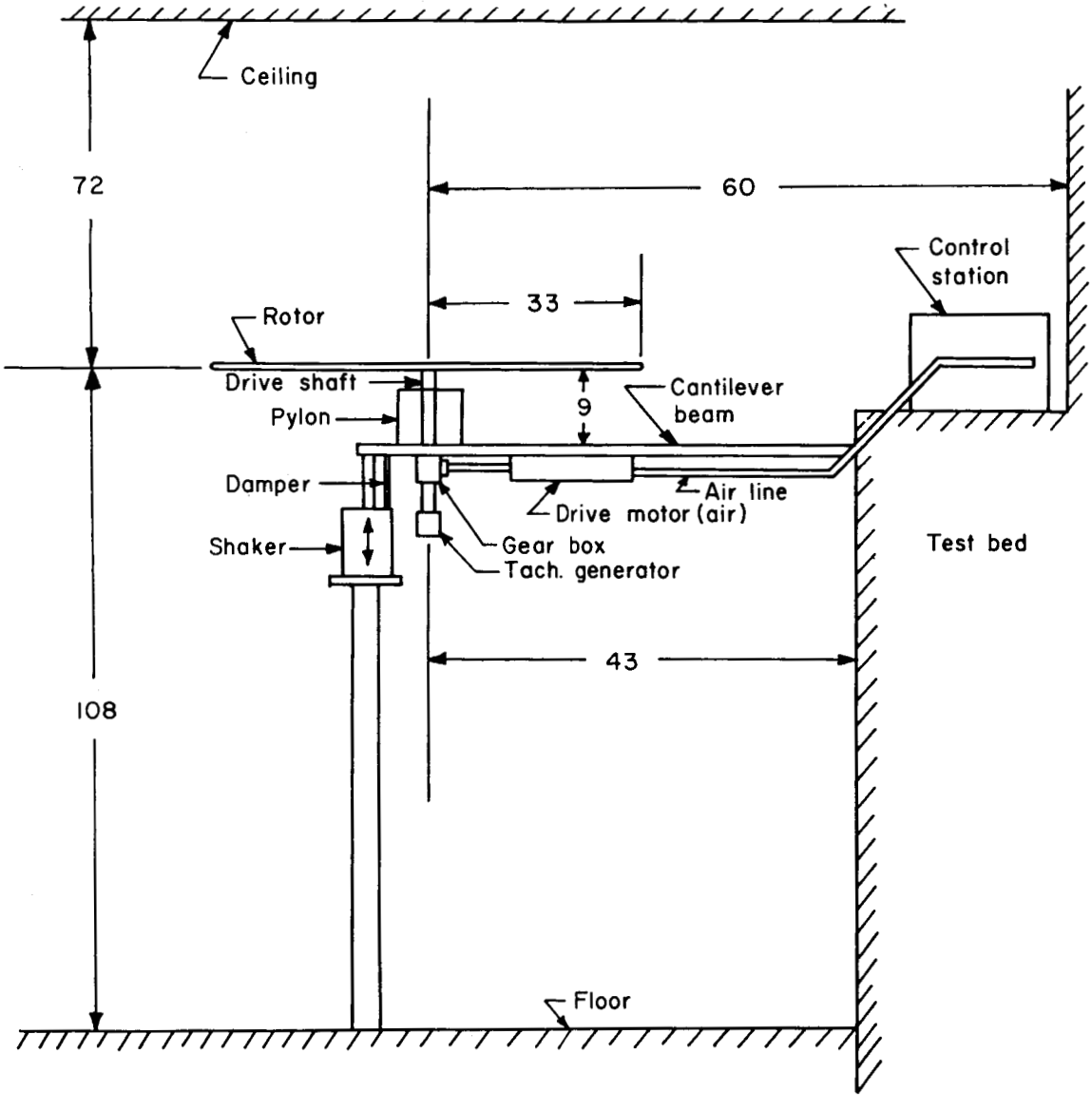

Figure 1.- General arrangement of test apparatus for teetering rotor. All dimensions are given in inches.

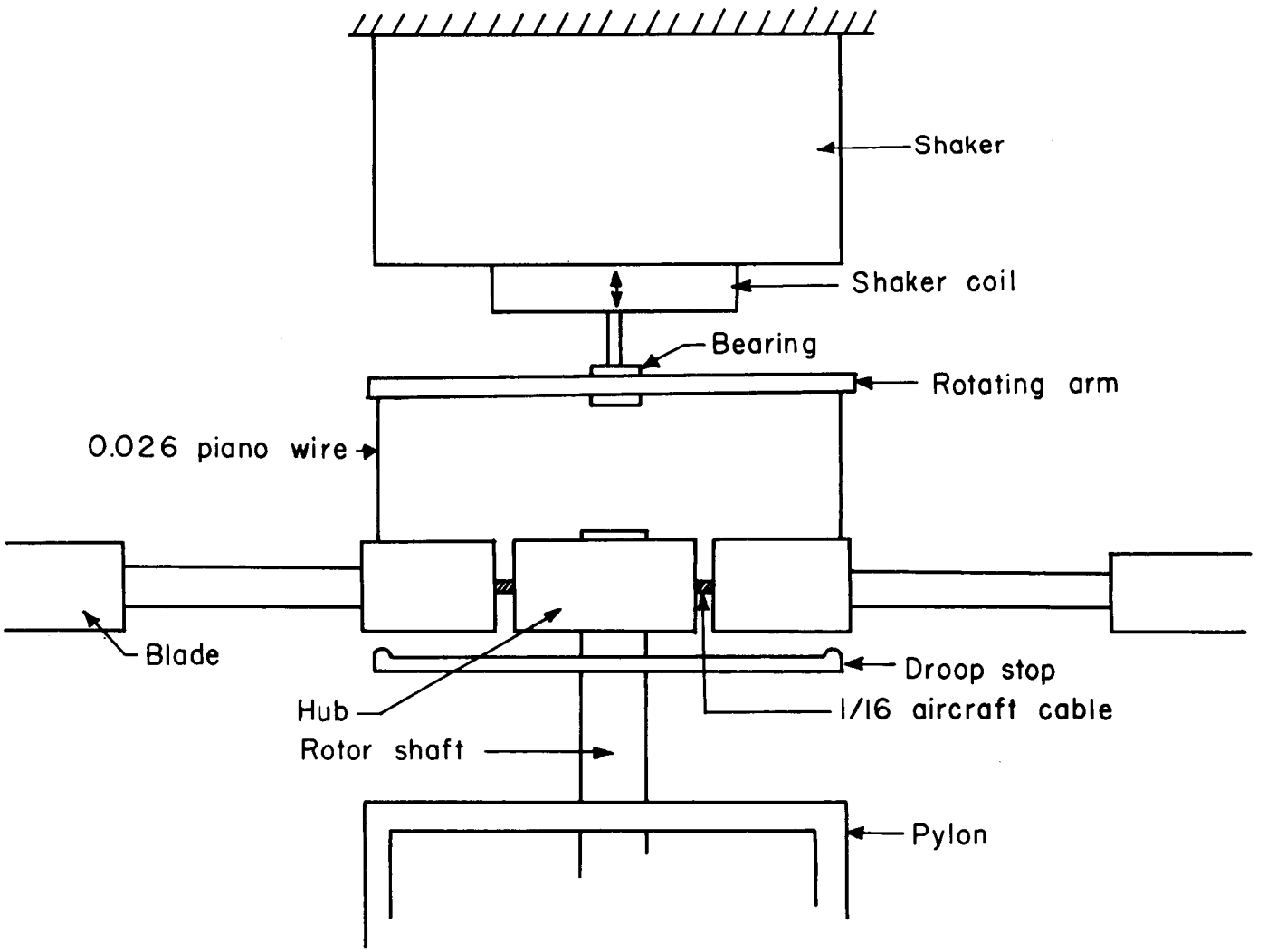

Figure 2.- Shaker arrangement for flapping rotor. All dimensions are given in inches.

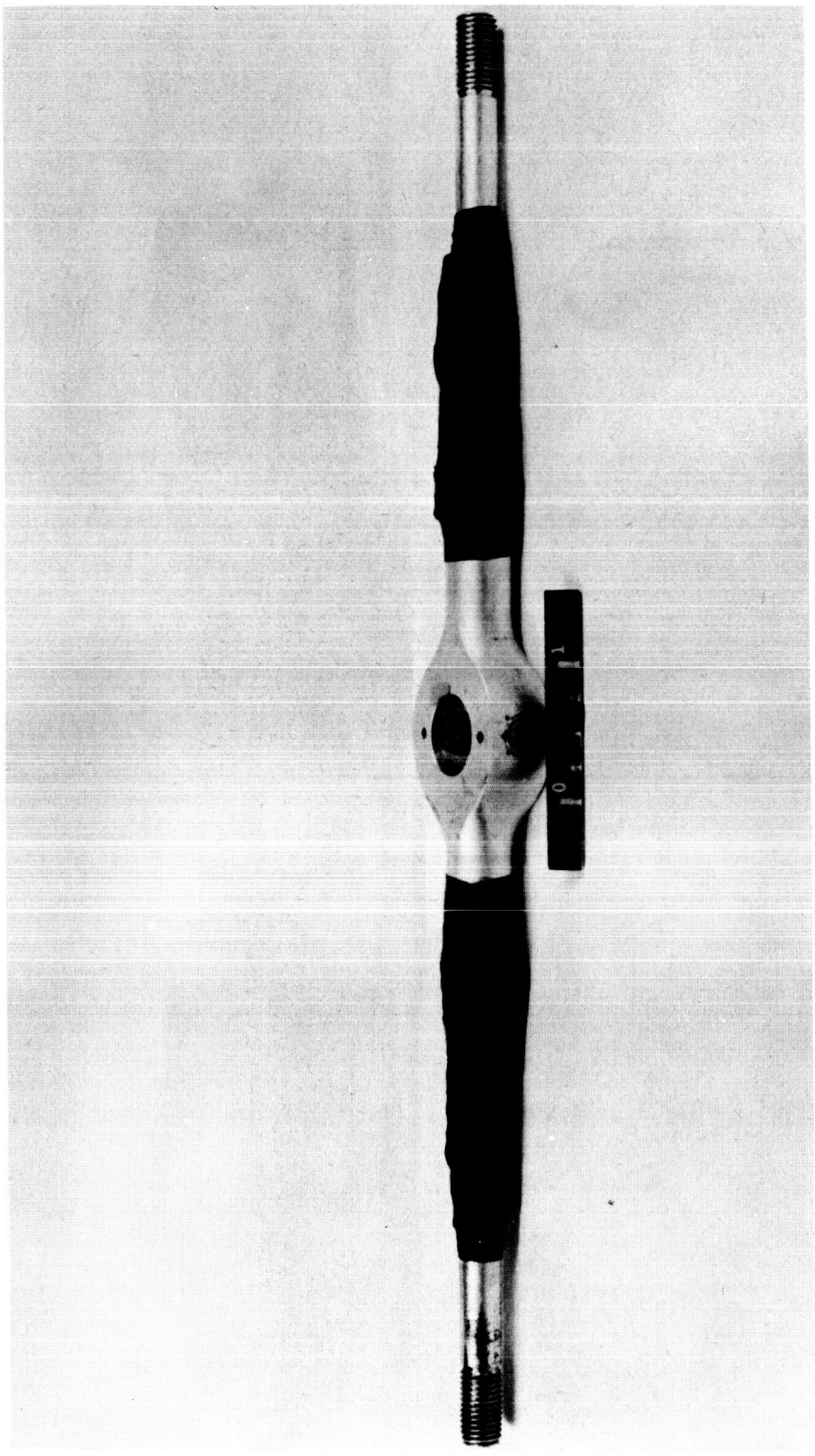

L-58-2700

Figure 3.- Teetering-rotor hub.

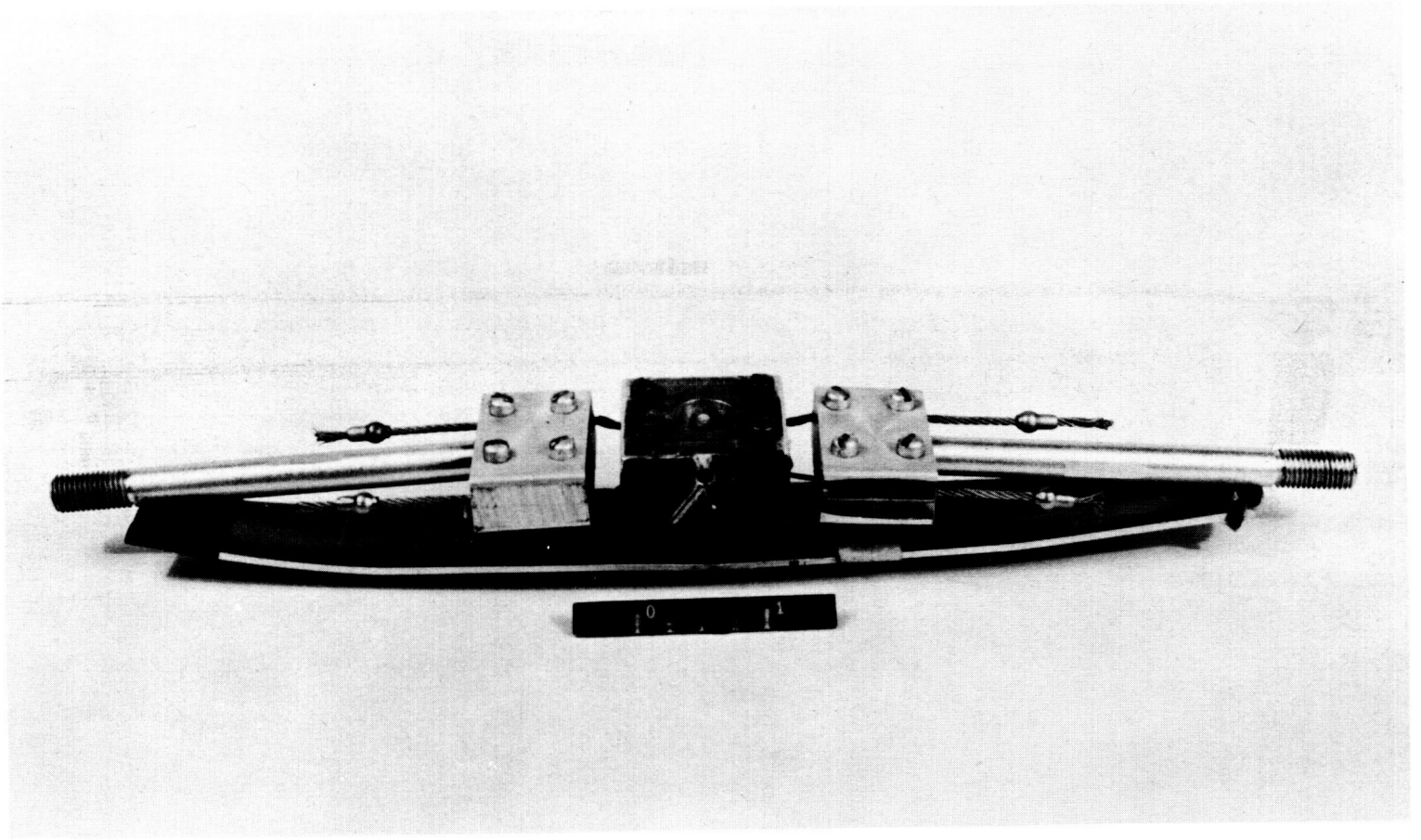

Figure 4.- Retention-strap flapping rotor. L-58-2702

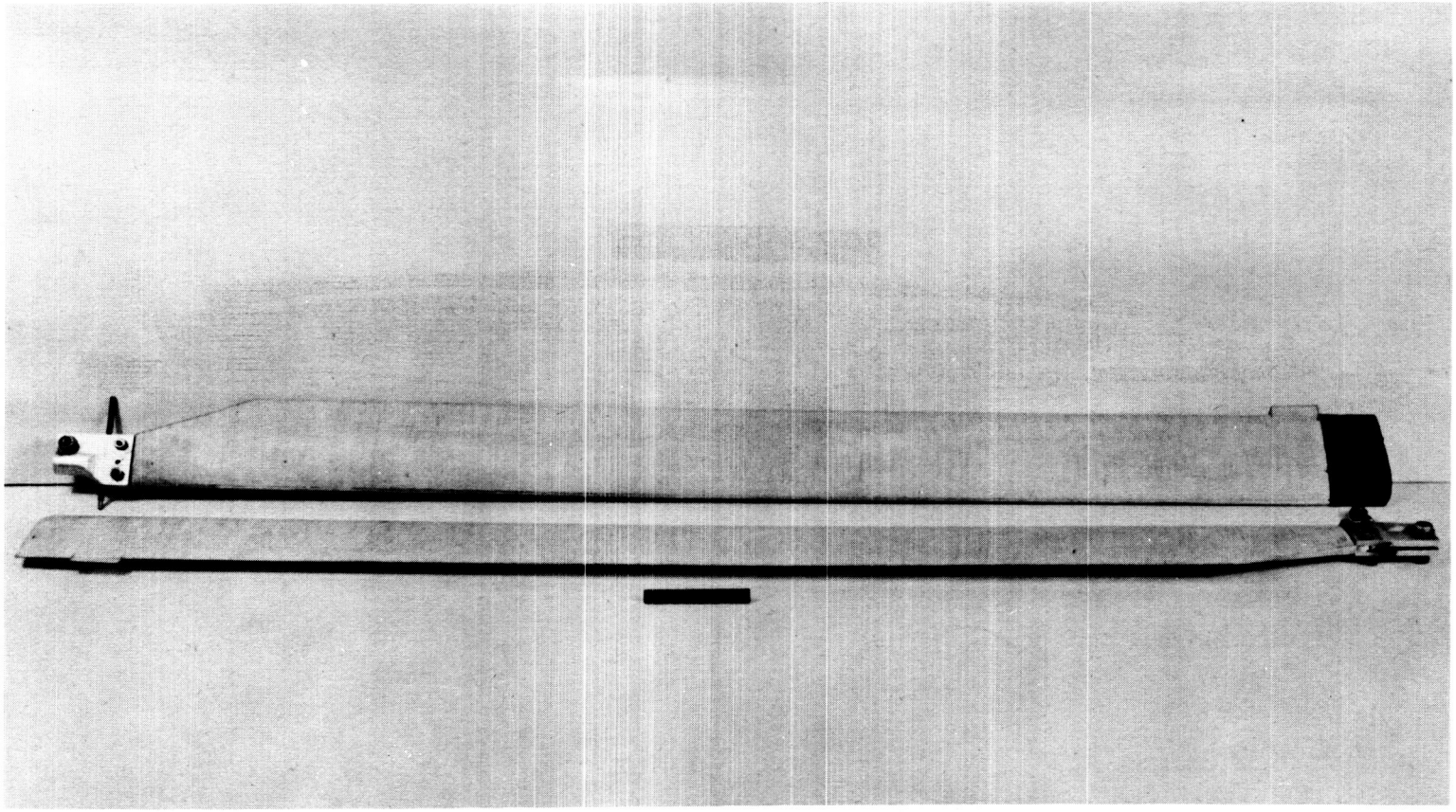

Figure 5.- Rotor blades. L-58-2696

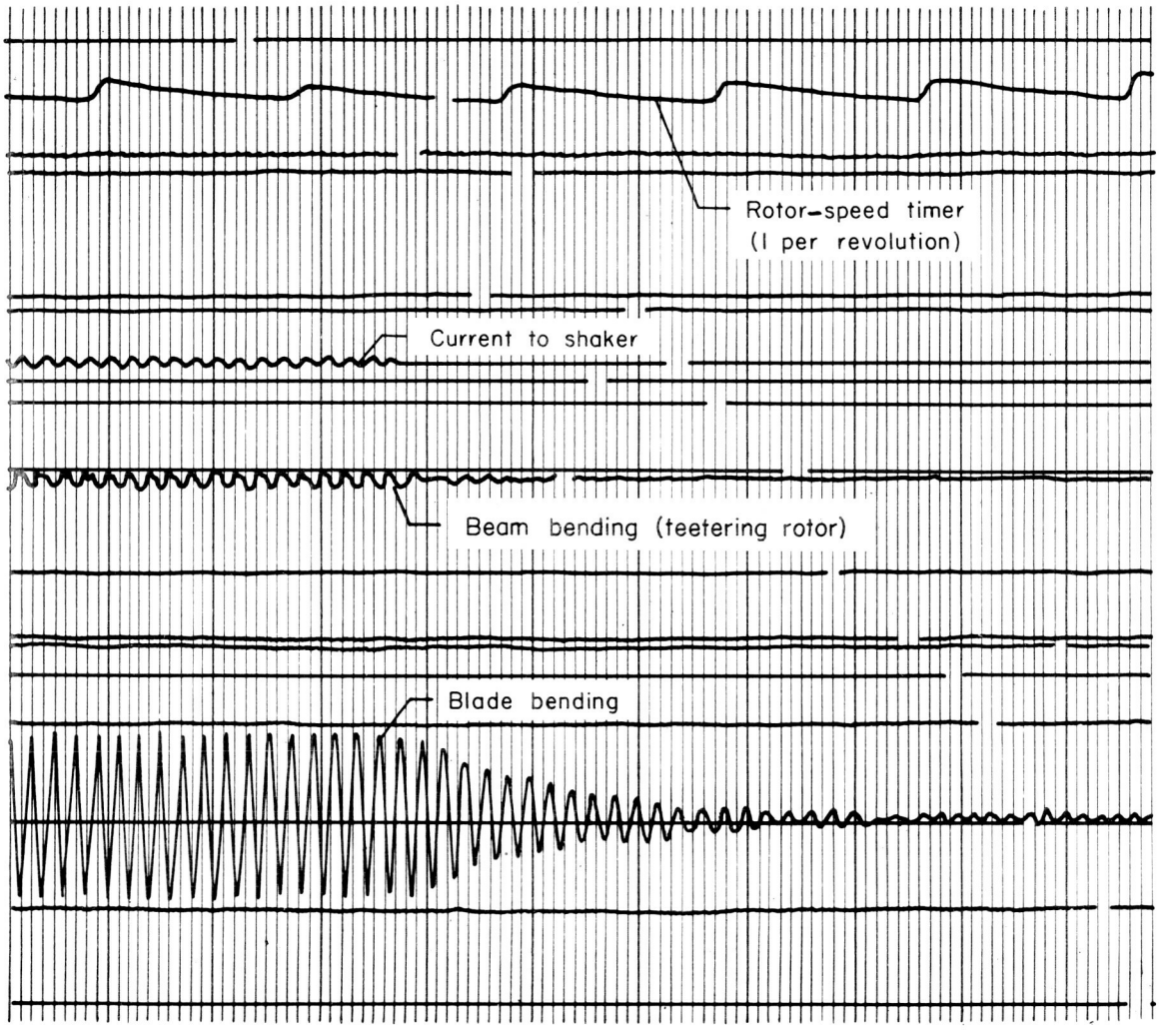

Figure 6.- Typical record showing traces of rotor-speed timer, shaker current, and bending of rotor blade.

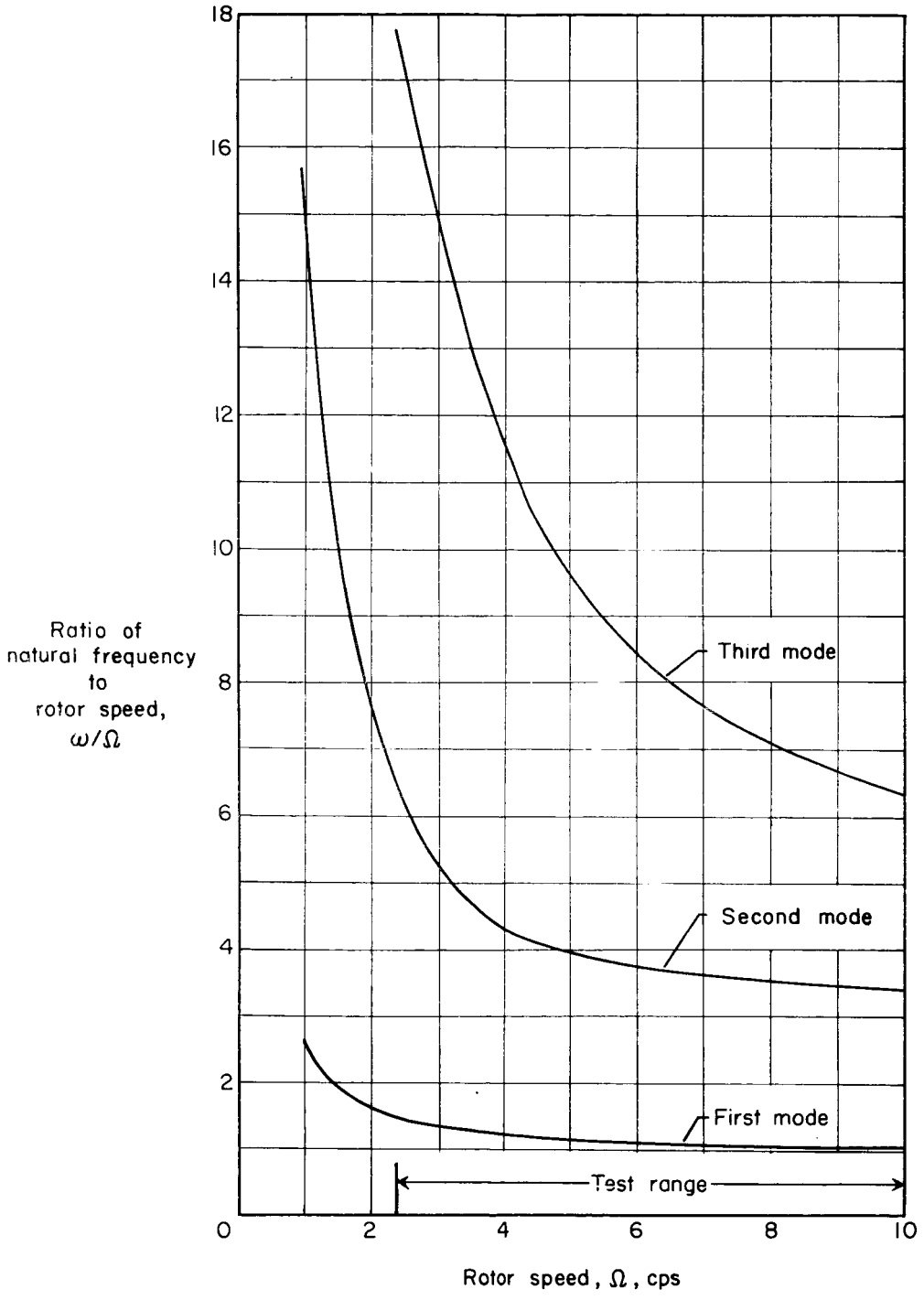

Figure 7.- Variation of flapwise bending frequencies with rotor speed for the teetering rotor. Symmetric modes.

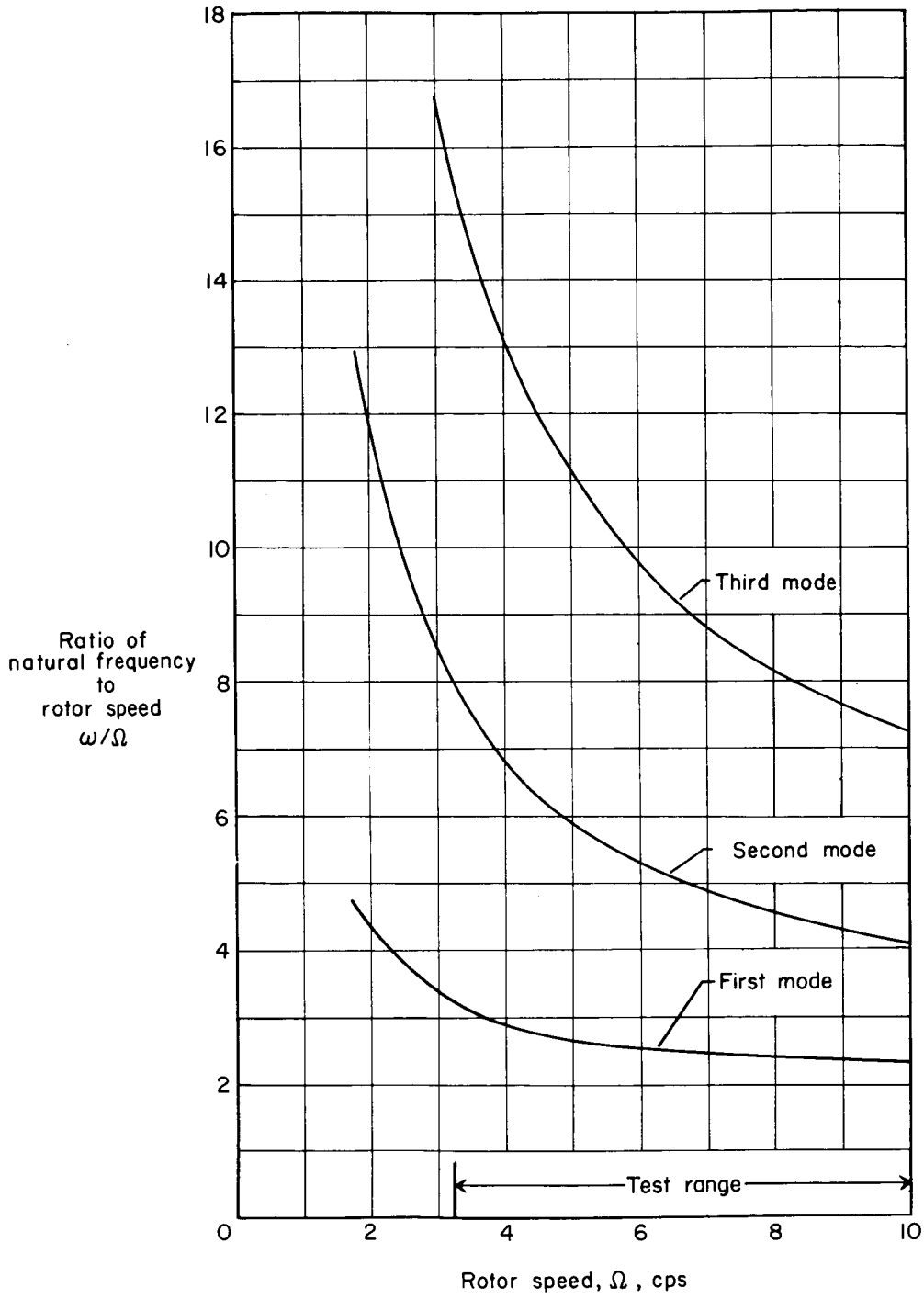

Figure 8.- Variation of flapwise bending frequencies with rotor speed for the retention-strap flapping rotor.

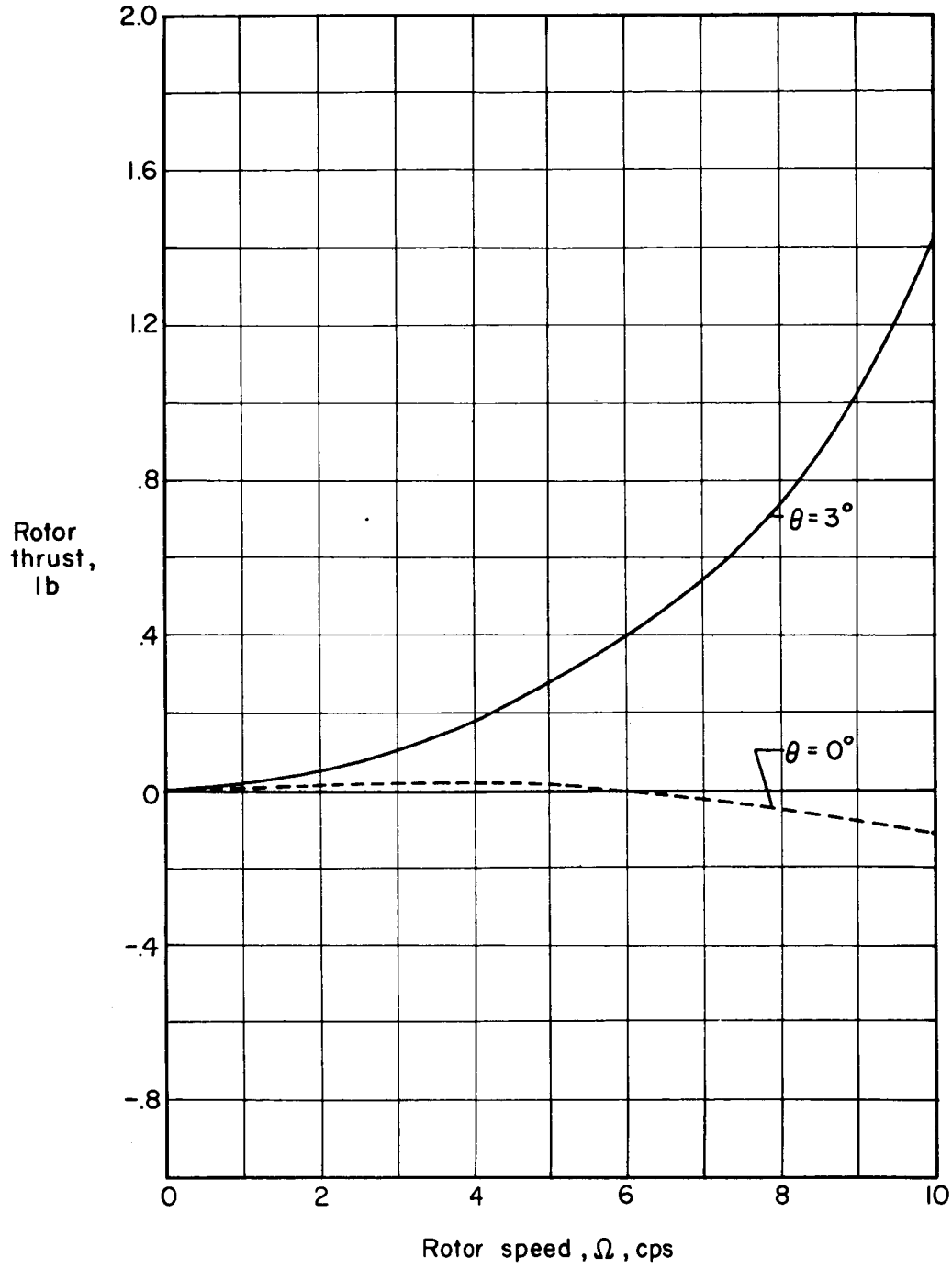

Figure 9.- Variation of rotor thrust with rotor speed for nominal collective pitch-angle settings of $\theta = 0^{\circ}$ and 3° for the teetering rotor.

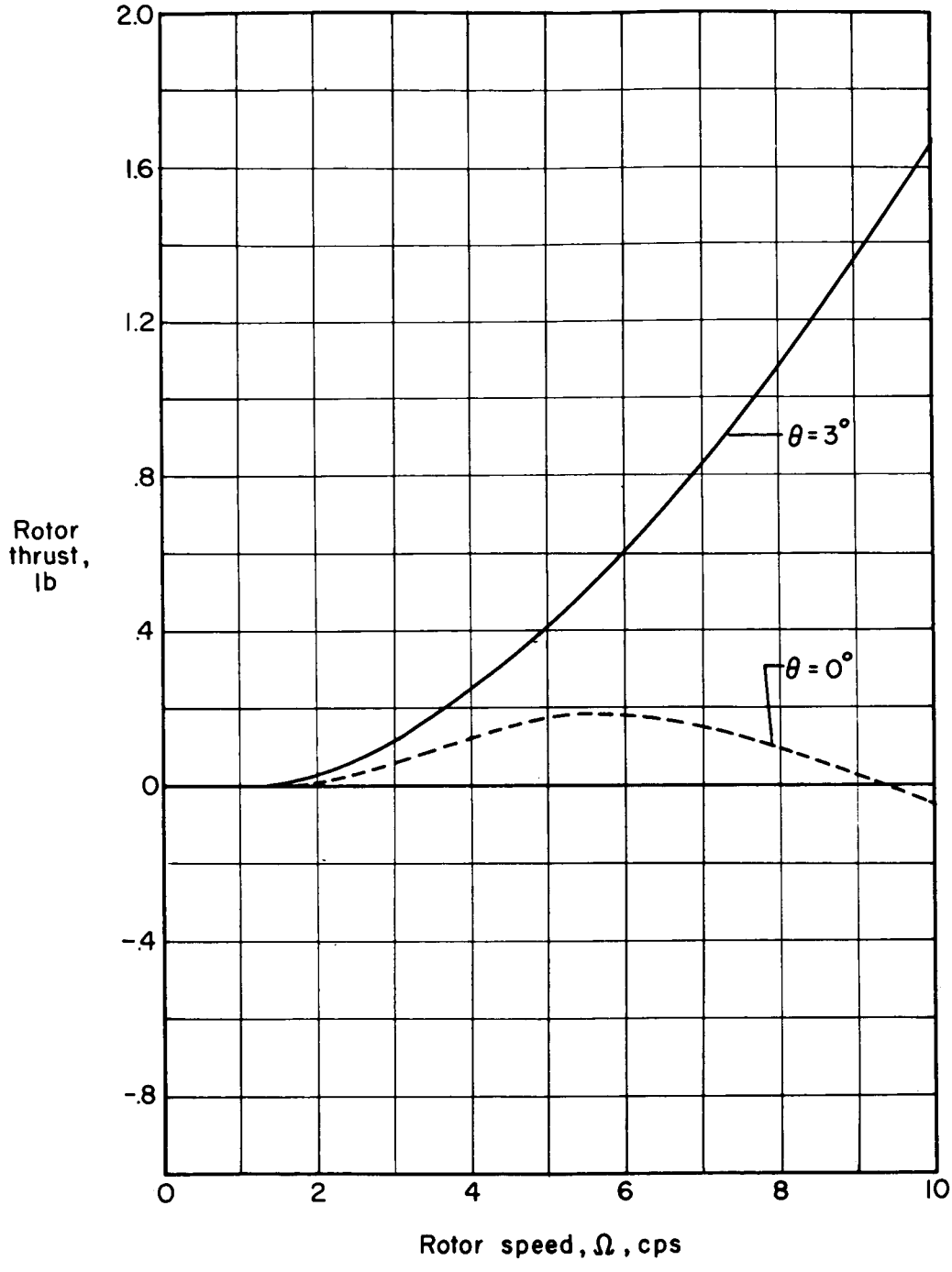

Figure 10.- Variation of rotor thrust with rotor speed for nominal collective pitch-angle settings of $\theta = 0^{\circ}$ and 3° for the retention-strap flapping rotor.

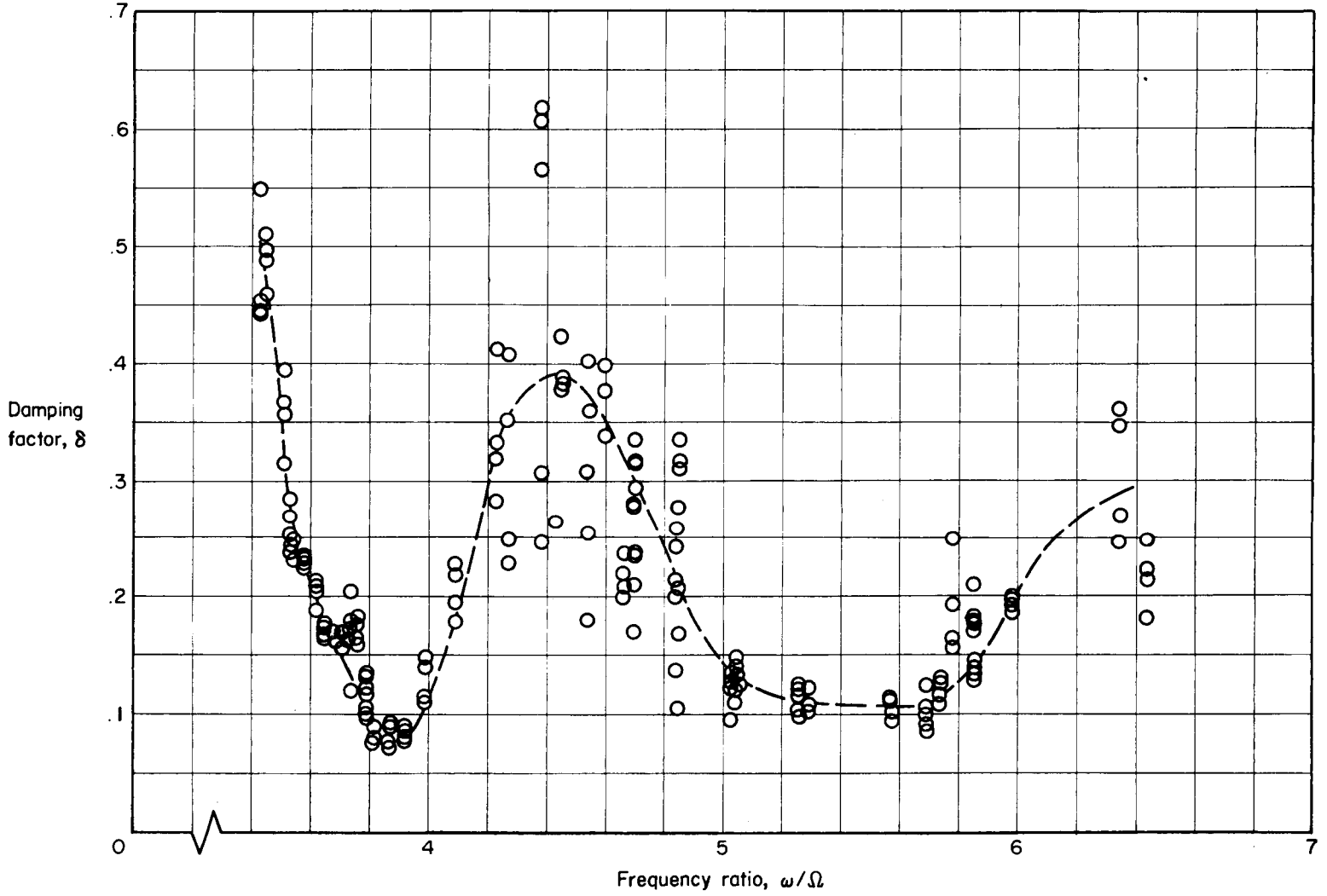

Figure 11.- Typical plot of experimental data points for the teetering rotor. Second mode; $\theta = 0^{\circ}$.

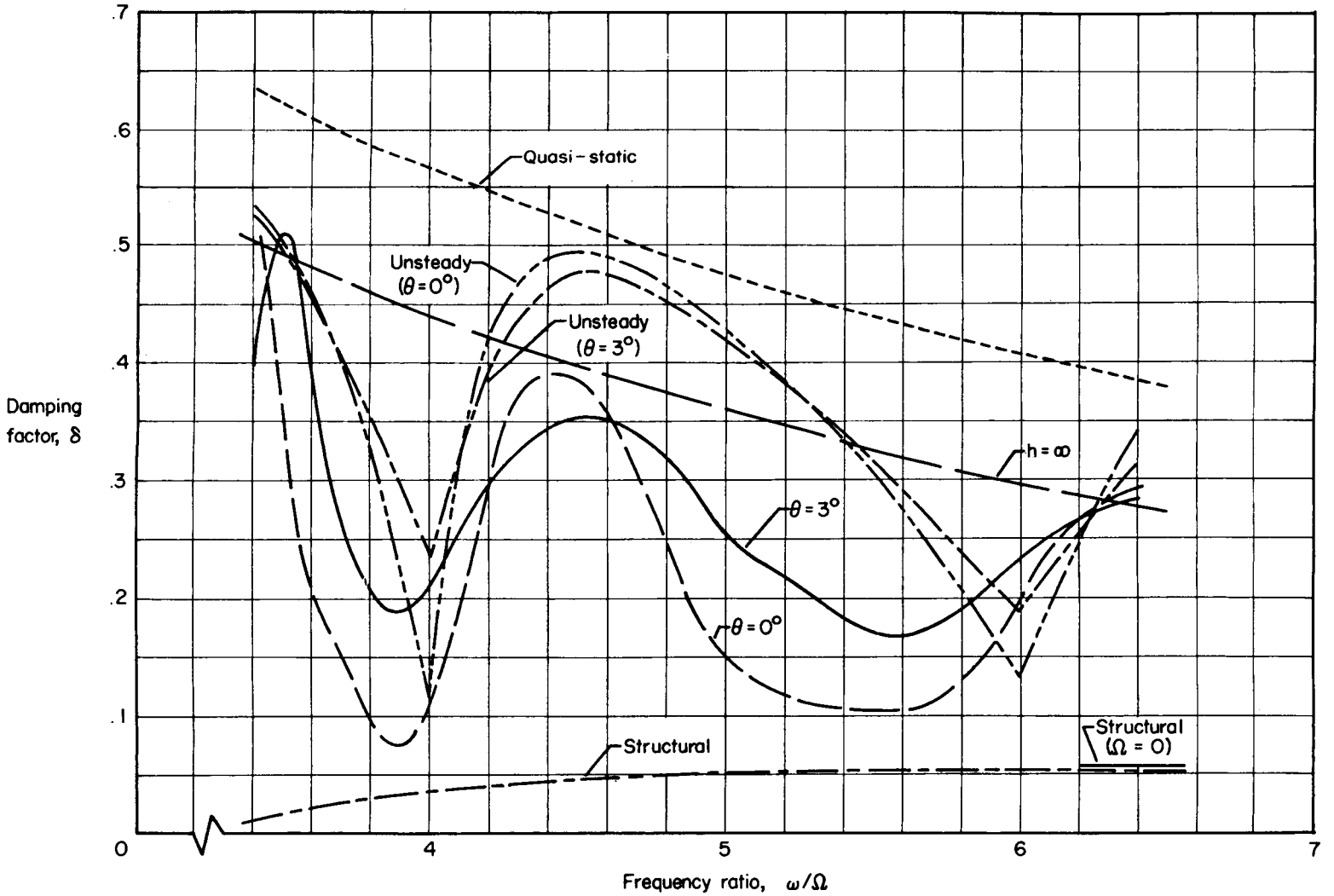

Figure 12.- Variation of damping factor with frequency ratio for the second elastic bending mode for the teetering rotor.

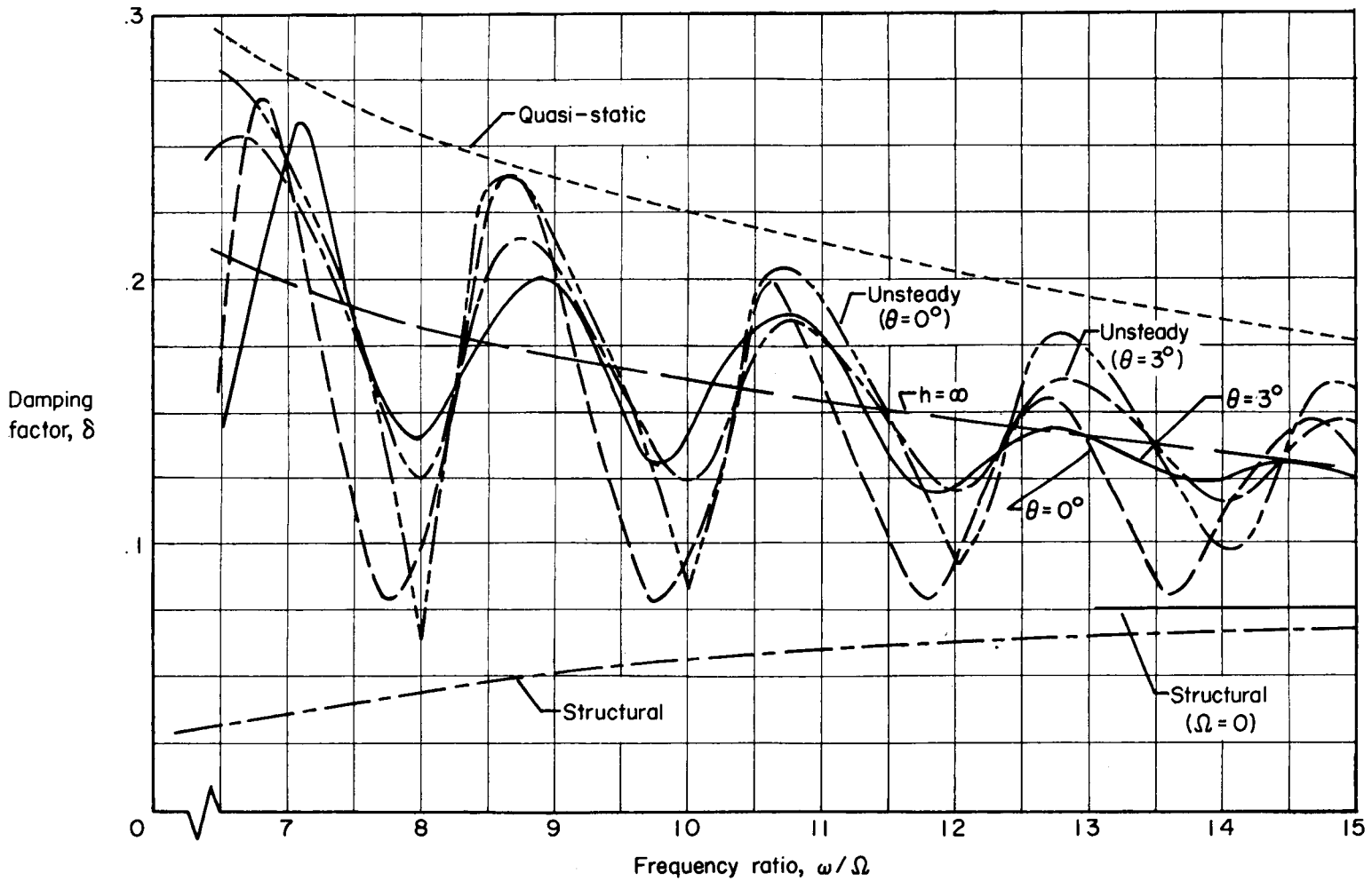

Figure 13.- Variation of damping factor with frequency ratio for the third elastic bending mode for the teetering rotor.

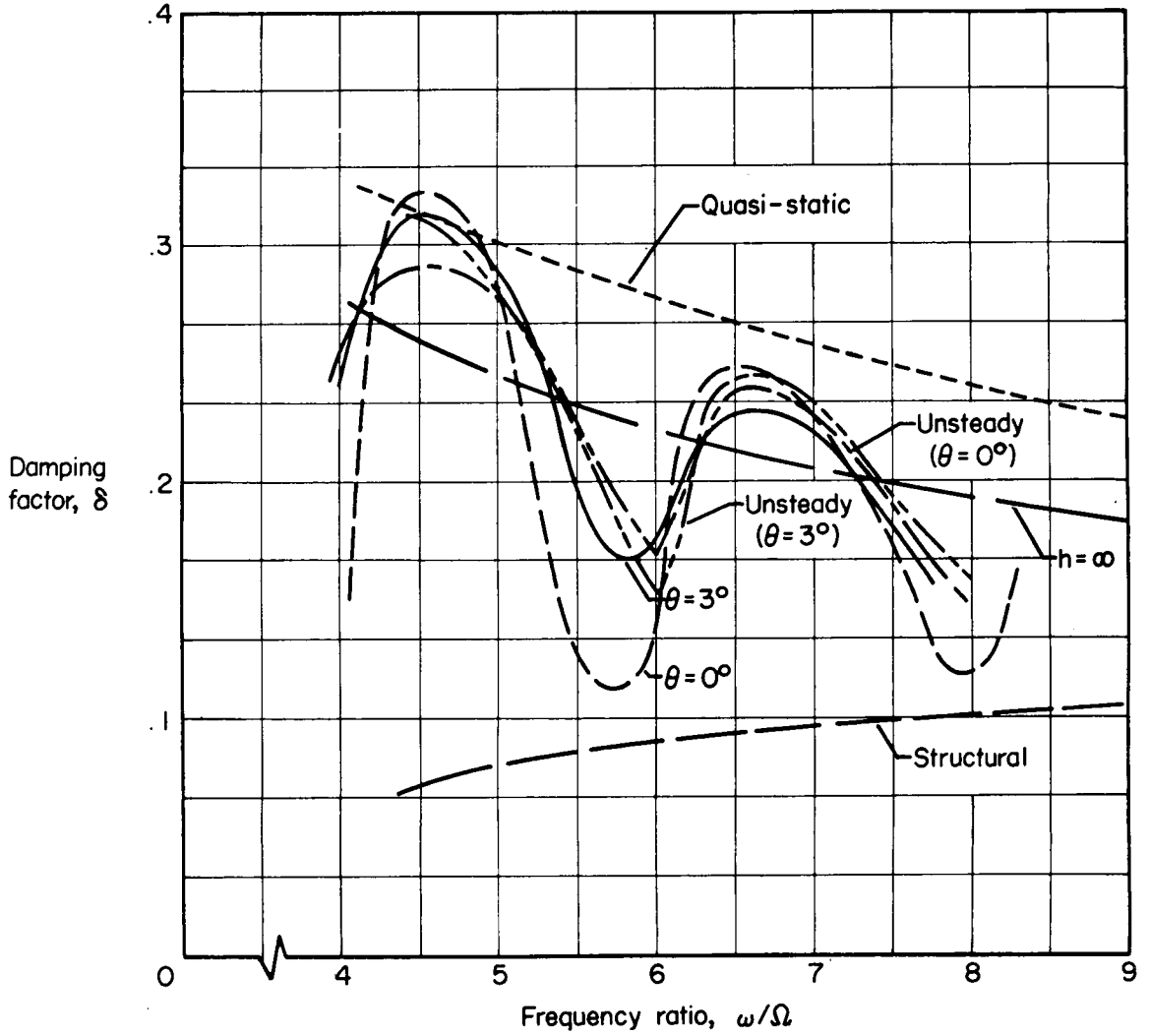

Figure 14.- Variation of damping factor with frequency ratio for the second elastic bending mode for the retention-strap flapping rotor.

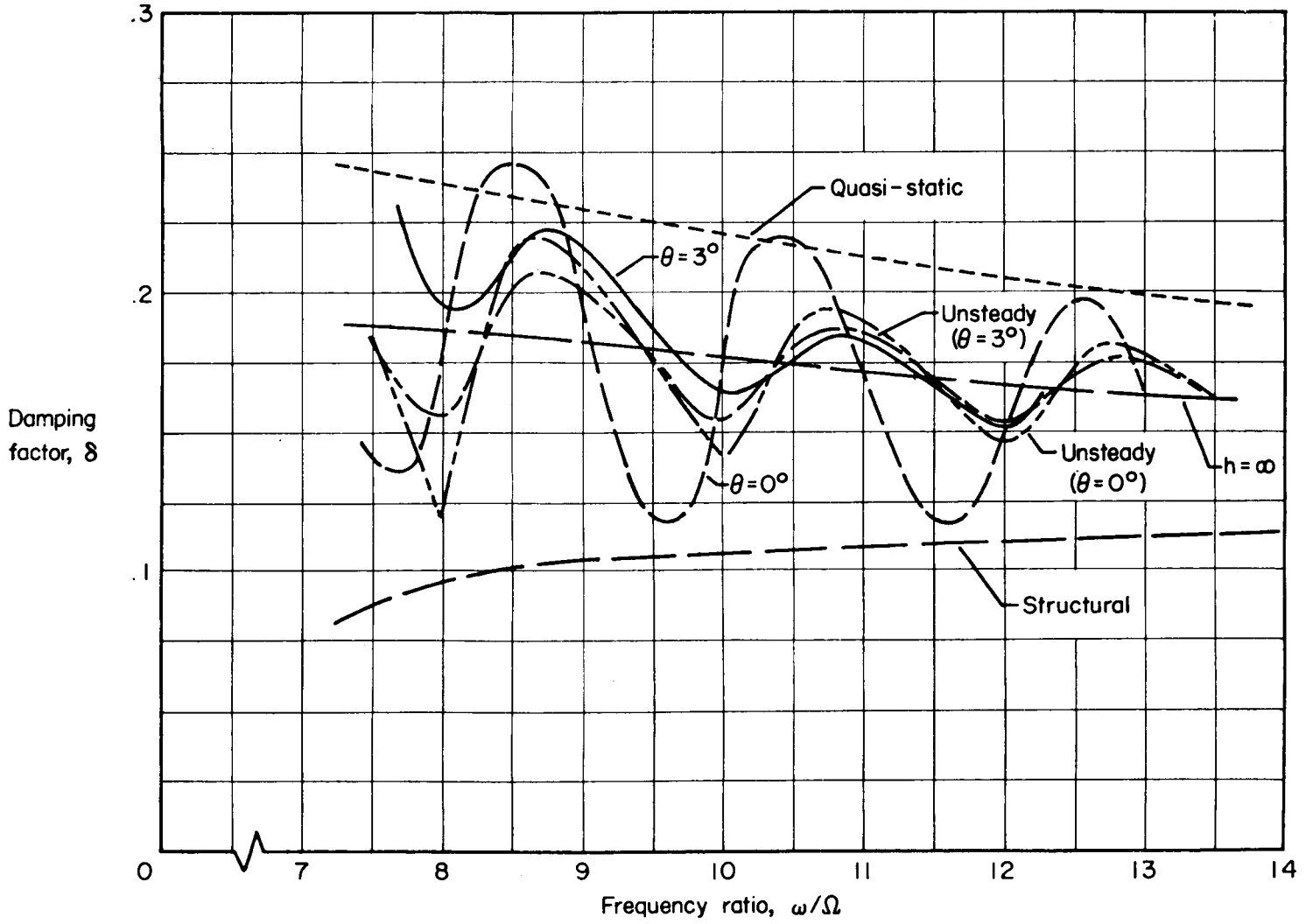

Figure 15.- Variation of damping factor with frequency ratio for the third elastic bending mode for the retention-strap flapping rotor.

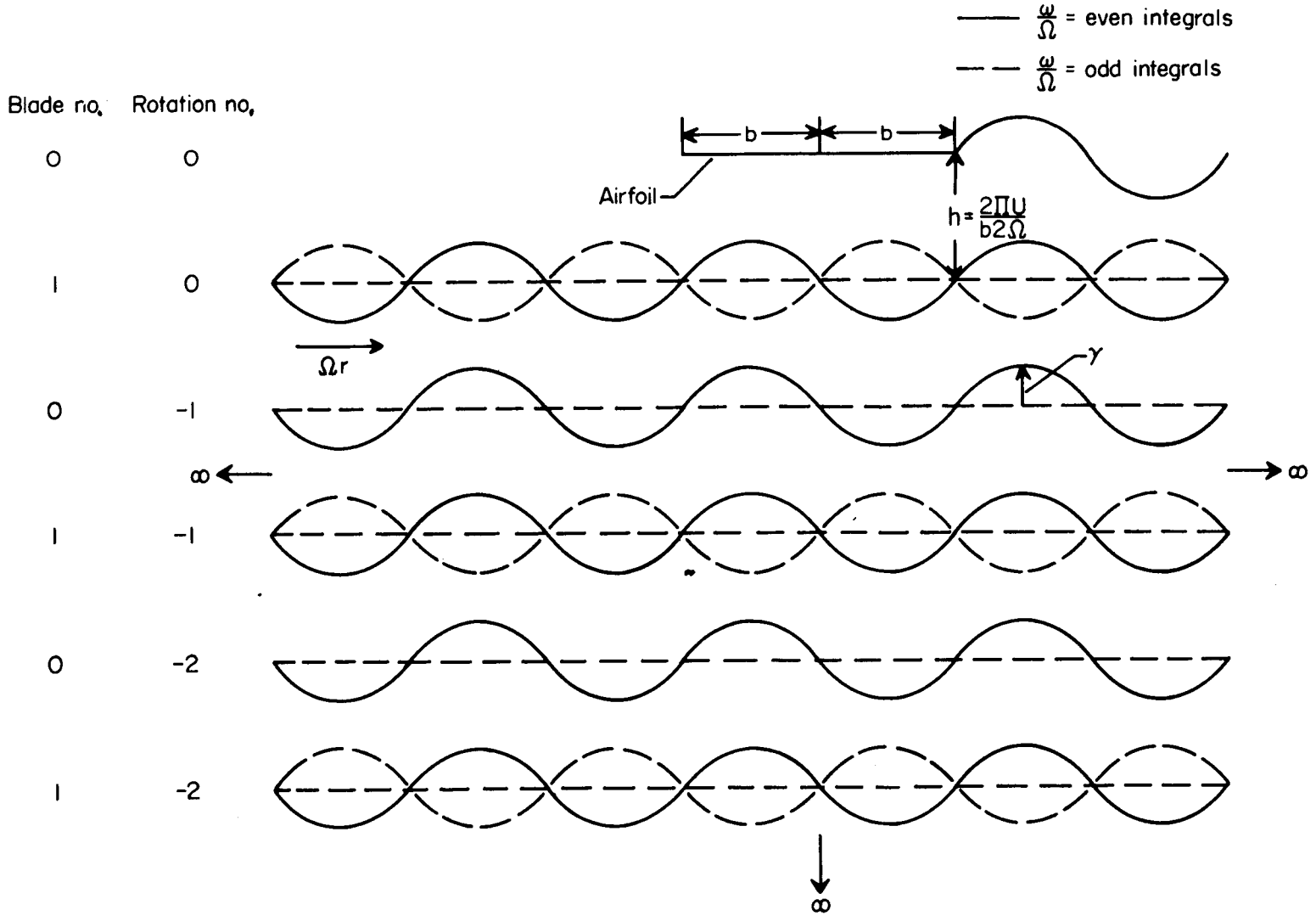

Figure 16.- Aerodynamic model for two-blade rotor. Symmetrical oscillations.